polysaccharides

MDPI

Article

Bacterial Cellulose Dressings from Mango Pulp Agro-Waste Functionalized with Grapefruit Seed Oil for Diabetic Wound Healing

Mayra E. García-Sánchez [1,2,3], Alfonso Barajas-Cervantes [2,†], Inés Jiménez-Palomar [1], José M. Acosta-Cuevas [2] and Erick O. Cisneros-López [2,*]

[1] inMateriis S.A. de C.V., Lerdo de Tejada #2334, Col. Americana, Guadalajara C.P. 44150, Mexico; mayra.garcia@inmateriis.com (M.E.G.-S.); ines.jimenez@inmateriis.com (I.J.-P.)
[2] Departamento de Física, Centro Universitario de Ciencias Exactas e Ingenierías, Universidad de Guadalajara, Blvd. Gral. Marcelino García Barragán #1421, Col. Olímpica, Guadalajara C.P. 44430, Mexico; jose.acosta@academicos.udg.mx (J.M.A.-C.)
[3] Laboratorio Nacional para la Investigación en Inocuidad Alimentaria LANIIA, Universidad Autónoma de Nayarit, Av. Emilio M. Gonzalez SN, Col. Ciudad del Conocimiento, Tepic C.P. 63173, Mexico
* Correspondence: erick.cisneros@academicos.udg.mx; Tel.: +52-33-13785900 (ext. 27668)
† Deceased author.

Abstract

Bacterial cellulose (BC) is an emerging biopolymer for skin tissue regeneration; however, its functionalization with natural antimicrobial agents remains limited. This study reports the preclinical evaluation of a BC-based dressing for diabetic wounds. BC membranes were obtained from mango pulp agro-waste by *Komagataeibacter xylinus* cultivation (6.32 g/L) and functionalized with grapefruit seed oil (GSO) at three v/v ratios (1:100, 1:200 and 1:500). FTIR spectroscopy confirmed GSO incorporation into the BC matrix through physical interactions, with a dose-dependent loading. Antimicrobial activity of the BC/GSO dressings was screened against *Staphylococcus aureus*, *Escherichia coli* and *Candida albicans* by agar diffusion, showing dose-dependent inhibition zones. Following the minimum effective dose principle, the BC/GSO 1:500 (v/v) formulation was selected for comprehensive biocompatibility evaluation (cytotoxicity, mutagenicity, pyrogenicity and sensitization) and for in vivo wound-healing testing in a streptozotocin-induced diabetic Wistar rat model. Cell viability above 70% was achieved from membrane-extract dilution 1:100,000, while mutagenicity, pyrogenicity and sensitization assays confirmed the absence of adverse biological responses. In vivo, BC/GSO 1:500 (v/v) dressings supported wound closure comparable to nitrofurazone, with no clinical signs of infection. Overall, these results position BC/GSO dressings as a sustainable, biocompatible and antimicrobial candidate for early-stage diabetic wound regeneration and demonstrate the technical feasibility of valorizing mango pulp agro-waste into a high-value biomedical biopolymer.

Keywords: bacterial cellulose; agro-waste valorization; grapefruit oil; antimicrobial wound dressing; diabetic foot ulcer; skin regeneration

Check for updates

Academic Editors: Tina Maver and Uroš Maver

Received: 27 March 2026
Revised: 19 May 2026
Accepted: 26 May 2026
Published: 15 June 2026

Copyright: © 2026 by the authors. Licensee MDPI, Basel, Switzerland. This article is an open access article distributed under the terms and conditions of the Creative Commons Attribution (CC BY) license.

1. Introduction

Cellulose is the most abundant polymer on Earth [1,2]. Its linear structure consists of 2000 to 14,000 β-(1,4)-linked glucose units held together by hydrogen bonds. It is a biopolymer with highly ordered regions (crystalline) and regions where the degree of

order is low (amorphous) [3,4]. Particularly, bacterial cellulose (BC) has recently attracted considerable interest for the development of high-value-added products [5,6].

BC is synthesized by several microorganisms, with *Komagataeibacter xylinus* being one of the most efficient producers [7–9]. This bacterium forms BC membranes as a flotation mechanism at the liquid/air interface, where it obtains the oxygen necessary for its growth. This membrane also acts as a physical barrier that protects the bacteria from UV radiation and toxic compounds, increases their ability to colonize substrates, and allows them to retain moisture [10,11]. Due to its high degree of crystallinity, purity, cross-linked structure, biodegradability, and biocompatibility, this polymer is attractive in various applications, especially in the medical area [12,13]; however, the high cost of conventional culture media has long limited the industrial scale-up of BC production [14,15].

Recent research has demonstrated the feasibility of producing this biopolymer from a wide range of agro-industrial waste streams, including fruit pulps and juices, molasses, bagasse and other lignocellulosic materials [16–18]. In Mexico, mango processing generates large volumes of pulp residues that are commonly discarded rather than valorized into value-added bioproducts [19]. Among the high-value-added bioproducts that can be obtained from BC, biomedical applications are particularly relevant. Its use has been reported in artificial blood vessels, scaffolds for cartilage and bone tissue engineering, drug-delivery matrices, and an outstanding range of applications in skin regeneration [20–22], particularly in chronic wounds associated with metabolic diseases.

Diabetes mellitus, one of the most prevalent chronic diseases worldwide [23,24], frequently leads to chronic wounds in which the normal phases of skin regeneration stall due to peripheral vascular disease, microvascular dysfunction and increased susceptibility to infection [25–27]. Among its most burdensome complications are diabetic foot ulcers (DFU), which account for most foot amputations in diabetic patients [28,29] and require prompt treatment with wound dressings that prevent further infection [30–32], provide a moist environment, and, when functionalized, deliver bioactive agents supporting the healing process [33].

BC has shown superior performance compared to traditional dressings such as gauze, which can adhere to the wound surface and cause trauma at the end of treatment [34]. BC facilitates tissue regeneration [35–37] and its high mechanical strength in the wet state, hydration capacity, retention of wound exudate, permeability to liquids and gases, low skin irritation and ability to absorb functional substances make BC membranes a useful material for the care and regeneration of cutaneous wounds [34,38–40], even superior to autografts in patients with severe skin damage [41–43]. These properties have driven the translation of BC from the laboratory to commercial wound-care products. Notable examples include Biofill® and Gengiflex® for covering wounds, Membracel® for burns and varicose ulcers, and Bioprocess® and XCell®, also topically applied for wound healing [41–46]. However, most commercial BC dressings remain non-functionalized and lack intrinsic antimicrobial activity.

Research has reported that BC can be combined with materials such as chitosan, polyethylene glycol (PEG), hydroxyapatite, polyvinyl alcohol (PVA), gelatin, and platelet-derived substances, among others, for a wide range of biomedical applications [36–39,42,43], consolidating BC as one of the most versatile platforms for advanced wound care. BC can be modified through chemical or physical post-production functionalization strategies, including the loading of antimicrobial agents to address the specific needs of chronic wounds [47].

Functionalized dressings with antimicrobial agents can reduce the risk of infection and improve healing; however, many of the active compounds currently used are very costly and difficult to regulate and control [48]. In this sense, the development of more efficient, less expensive, biocompatible and biodegradable dressings functionalized with

bioactive compounds is preferred [49], as they can overcome the toxicity, mutagenicity and bacterial resistance associated with traditional antimicrobials [50].

In recent decades, essential oils have been studied as natural active substances with antimicrobial activity against various pathogenic microorganisms [51–53], including pharmacological properties such as bacteriostatic effects, free radical scavenging activity, anti-inflammatory activity, and tumor cell inhibition [54]. Among plant-derived essential oils, grapefruit seed oil (GSO) exhibits antifungal, antiparasitic, antibacterial, antioxidant, and anticancer properties, and inhibits the growth of both Gram-positive and Gram-negative bacteria [55]. As with most citrus oils, GSO is mainly composed of terpene-derived compounds responsible for its characteristic aroma, as well as terpene oxides including alcohols, ethers, aldehydes, ketones, and esters [12]. Recent research has focused on the use of GSO for the treatment of certain diseases and tissue regeneration [56], for which preclinical laboratory studies are required prior to clinical translation [57].

Within the framework of modern biotechnology, which involves multidisciplinary research with impact on public health as well as on environmental, economic and industrial sectors [58,59], the present work addresses three converging challenges: the integration of mango pulp agro-waste valorization with biomedical-grade BC production through cultivation of *K. xylinus*, the functionalization of BC membranes with grapefruit seed oil (GSO) at three v/v ratios as a natural antimicrobial alternative, and the comprehensive preclinical safety and efficacy evaluation required for translational progression of medical-device candidates, covering in vitro and in vivo assays. Overall, this work aims to position BC/GSO dressings as a sustainable, biocompatible and antimicrobial candidate for early-stage diabetic wound regeneration.

2. Materials and Methods

2.1. Materials

Mango pulp agro-waste (MPW) was obtained from Tommy Atkins mango cultivated in Amatitán, Jalisco (Mexico) and processed as previously described [60]. The bacterial strain used for BC production was *Komagataeibacter xylinus* DSMZ 2004, obtained from the German Collection of Microorganisms and Cell Cultures (DSMZ, Braunschweig, Germany). Yeast extract used as a nitrogen source in the culture medium was supplied by MCD-Lab (Tultitlán, Mexico). Sodium hydroxide (NaOH) and ethanol (96%, analytical grade) used for membrane purification and handling were purchased from Golden Bell (Guadalajara, Mexico). Grapefruit seed oil (GSO, 99%) used for BC functionalization was purchased from Young Living (Lehi, UT, USA).

For in vitro antimicrobial assays, Mueller–Hinton agar was supplied by Golden Bell (Guadalajara, Mexico), and gentamicin discs (10 µg/disc) were used as a positive control. The bacterial strains *Staphylococcus aureus* (ATCC 6538), *Escherichia coli* (ATCC 8739), and *Candida albicans* (ATCC 10231) were used as test microorganisms. For cytotoxicity assays, the NIH/3T3 fibroblast cell line (ATCC CRL-1658, Manassas, VA, USA) was used. For in vivo studies, streptozotocin (Sigma-Aldrich, St. Louis, MO, USA) was used to induce diabetes in Wistar rats, and nitrofurazone (Furacin®, 2 mg/g) was used as the reference wound-healing treatment. For biocompatibility assays, endotoxin-free water, cisplatin and methyl methanesulfonate (MMS) were purchased from Sigma-Aldrich (St. Louis, MO, USA). All other reagents were of analytical grade.

2.2. Methods

2.2.1. BC Production

BC membranes were produced by static cultivation of *K. xylinus* using mango pulp waste (MPW) as the carbon source. The MPW-based culture medium was prepared with

a total sugar concentration of 50 g/L (30 g/L sucrose, 15 g/L glucose, 5 g/L fructose), supplemented with 10 g/L yeast extract as nitrogen source, 2.7 g/L Na_2HPO_4 and 1.15 g/L citric acid as a buffer, and adjusted to pH 6.5. A control medium based on the standard Hestrin–Schramm (HS) formulation was prepared with the same sugar mixture instead of pure glucose, 5 g/L peptone, 5 g/L yeast extract, 2.7 g/L Na_2HPO_4 and 1.15 g/L citric acid. Both media were sterilized at 121 °C for 7 min prior to inoculation.

The inoculum was prepared from a frozen stock of *K. xylinus* DSM 2004 propagated in liquid HS medium at 30 °C for 48 h under static conditions. Fermentation flasks (100 mL glass containers, 10 cm diameter) were filled with 20 mL of culture medium, inoculated, and incubated at 30 °C under static conditions for 16 days. After cultivation, BC membranes were harvested from the air–liquid interface, rinsed with distilled water and purified by immersion in 0.1 M NaOH at 90 °C for 30 min to remove residual cells and culture medium components. Membranes were then washed repeatedly with distilled water until the wash water reached neutral pH.

Purified membranes were freeze-dried at −45 °C and 0.8 MPa for 24 h (Freezone 4.5, Labconco, Kansas City, MO, USA) to preserve the reticular structure of BC and improve subsequent oil diffusion during rehydration. Dried membranes were stored in a desiccator until use. Detailed methodology, including kinetic and physicochemical characterization of MPW-derived BC, has been previously reported by García-Sánchez et al. [60].

2.2.2. Functionalization of BC Membranes with GSO

GSO solutions were prepared by dissolving GSO in ethanol at three volumetric ratios: 1:100, 1:200 and 1:500 (v/v). Lyophilized BC membranes were rehydrated by immersion in 20 mL of each GSO solution and vortexed at 3200 rpm for one minute, to promote uniform penetration of GSO into the porous BC network. Rehydrated membranes were cut into pieces of 1.5 cm^2 for in vitro antimicrobial assay and 3 cm^2 for in vivo healing tests, and transferred to test tubes containing 1.5–2 mL of the corresponding GSO solution. Test tubes were placed in a vacuum oven at 40 °C and 0.08 MPa for 24–30 h to evaporate the ethanol while retaining GSO within the membrane network.

After vacuum drying, each functionalized membrane was transferred to a 2 mL Eppendorf tube and extended along the wall to ensure uniform geometry. Samples were frozen at −80 °C and freeze-dried at −50 °C and 0.2 bar for 24 h. Functionalized BC/GSO membranes were stored in a desiccator until use. Cytotoxicity, mutagenicity, pyrogenicity and sensitization assays were performed using extracts obtained from these membranes, as described in corresponding subsections.

2.2.3. FTIR Characterization of BC/GSO Membranes

The chemical structure of pure GSO, non-functionalized BC, and BC/GSO membranes at 1:100, 1:200 and 1:500 (v/v) ratios was analyzed by Fourier-transform infrared spectroscopy (FTIR). Spectra were performed on a Nicolet iS50 FT-IR spectrometer (Thermo Scientific, Waltham, MA, USA) equipped with a diamond ATR accessory. Membrane samples were taken directly from the desiccator and analyzed in their dry state. Each spectrum was recorded over the 500–4000 cm^{-1} range with a resolution of 4 cm^{-1} and 32 scans.

2.2.4. Antimicrobial Activity Tests

Antimicrobial activity of BC/GSO membranes was tested in vitro by the agar diffusion method described by Woods [61], following the Kirby-Bauer diffusion principle. Functionalized BC/GSO membranes (1.5 cm^2) at 1:100, 1:200 and 1:500 (v/v) GSO ratios were tested against *Staphylococcus aureus* (ATCC 6538), *Escherichia coli* (ATCC 8739), and *Candida albicans* (ATCC 10231). Non-functionalized BC membranes were used as a negative control and gentamicin discs (10 µg/disc) as a positive control.

Bacterial and fungal suspensions were prepared from fresh cultures and adjusted to 0.5 McFarland (~1.5 × 10^8 CFU/mL) in sterile saline solution. Each suspension was inoculated onto Mueller–Hinton agar plates using a sterile cotton swab streaked in three directions to ensure a uniform lawn. The samples were placed at the center of each plate. Incubation conditions were 37 °C for 18 h for bacterial strains and 24 h for *C. albicans*. The radius of the inhibition zone was measured with a digital vernier caliper (Figure 1), and results are reported as mean ± standard deviation.

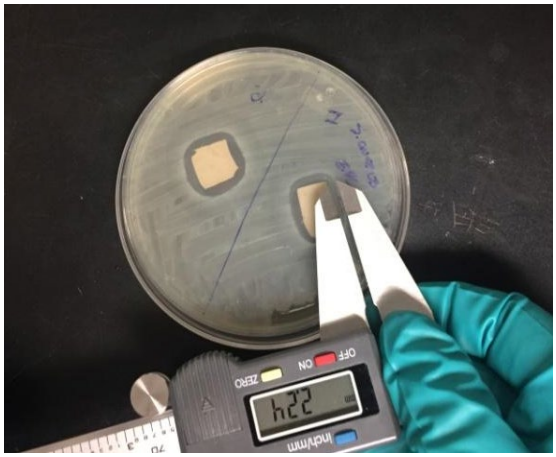


Figure 1. Measurement of the inhibition zone radius around BC/GSO membrane samples using a digital vernier caliper, performed in triplicate per microorganism (n = 3).

2.2.5. Cytotoxicity and Mutagenicity

Among the three formulations tested for antimicrobial activity, the BC/GSO 1:500 (v/v) dressing was selected for biocompatibility evaluations in accordance with the minimal effective dose principle. This formulation was therefore used for cytotoxicity, mutagenicity, pyrogenicity and sensitization assays. Sample preparation followed ISO 10993-12:2021 [62]: BC/GSO 1:500 (v/v) dressings were placed in endotoxin-free water at a ratio of 0.2 g/mL and incubated at 37 °C for 24 h to obtain the extract.

The extract was then serially diluted in endotoxin-free water by a factor of 10 to obtain 1:1000, 1:10,000, 1:100,000 and 1:1,000,000 dilutions, which were used as test solutions for cytotoxicity (MTT assay). For mutagenicity (Ames test), the BC/GSO 1:500 (v/v) undiluted extract was used.

Cytotoxicity was assessed according to ISO 10993-5:2009 [63] using the NIH/3T3 mouse embryonic fibroblast cell line (ATCC CRL-1658). Cells were maintained in DMEM with 10% fetal bovine serum at 37 °C and 5% CO_2. For the assay, cells were seeded into 96-well plates at 1 × 10^4 cells/well and exposed to each extract dilution for 24 h. Cell viability was determined by the MTT assay (absorbance at 570 nm). Untreated cells served as a negative control (100% viability) and cisplatin (12.5–200 µg/mL) as a positive control. Following ISO 10993-5:2009 [63], viability below 70% was considered cytotoxic. The assay was performed as a single experiment without replicates.

Mutagenicity was assessed by the Ames test according to ISO 10993-3:2014 [64], using *Salmonella typhimurium* strain TA100, which carries a base-pair substitution mutation in the histidine biosynthetic pathway, allowing the detection of mutagenic activity of the compounds. The lyophilized strain was rehydrated and pre-incubated at 37 °C for 16–18 h. Samples of BC/GSO 1:500 (v/v) extract were mixed with the bacterial culture and plated on minimal agar medium lacking histidine. Plates were incubated at 37 °C for 48 h, and the number of revertant colonies was recorded. Methyl methanesulfonate (MMS) was used as a positive control, while the extraction vehicle (endotoxin-free water) was used as a negative control. Results are reported as mean ± standard deviation of three plates per condition.

2.2.6. Pyrogenicity Test

The pyrogenicity test was performed on rabbits in accordance with MGA Method 0711 of the Medical Device Supplement to the Mexican Pharmacopeia [65]. The BC/GSO 1:500 (*v*/*v*) undiluted extract, prepared as described in Section 2.2.5, was used as the test solution. The protocol for the use of animals was approved by the Internal Committee for the Care of Laboratory Animals of CIATEJ, A.C.

Three New Zealand albino rabbits (*Oryctolagus cuniculus*) weighing 2.7 to 2.9 kg were housed in individual cages under controlled temperature and humidity conditions. The animals were fed a Purina balanced pellet diet and had access to purified water ad libitum. Feed was withdrawn 18 h before the test. On the day of the experiment, the weight of each rabbit was recorded. The rabbits were placed in individual restrainers, and rectal temperature was measured using a Welch Allyn SureTemp Plus electronic thermometer (Skaneateles Falls, NY, USA). A schematic representation of the experimental setup is provided in Figure S1 (Supplementary Materials).

Temperature recordings were taken for 3 h prior to administration of the test solution. The last temperature recorded (3 h) corresponded to the control temperature. 30 min after recording the control temperature, the BC/GSO extract was injected into the marginal ear vein at a volume of 1 mL/kg of body weight for each rabbit. Subsequently, the temperature of each animal was recorded every 30 min for 3 h. The maximum temperature for each rabbit corresponded to the highest temperature recorded within 3 h after injection. The test was considered negative when the temperature increase in each rabbit did not exceed the limits established by the Mexican Pharmacopeia.

2.2.7. Sensitization Test

The test was performed on guinea pigs in accordance with ISO 10993-10:2010 [66], using the Guinea Pig Maximization Test (GPMT) described by Magnusson and Kligman [63]. The protocol for the use of animals was approved by the Internal Committee for the Care of Laboratory Animals of CIATEJ, A.C.

Fifteen male Hartley guinea pigs with an average weight of 210 g were allocated to a treatment group (n = 10) and a control group (n = 5). Animals were housed in individual cages in a vivarium under controlled temperature and humidity, fed a balanced guinea pig pellet formula, and had access to purified water ad libitum. Feed was withdrawn 18 h before the test. The BC/GSO 1:500 (*v*/*v*) undiluted extract, prepared as described in Section 2.2.5, was used as the test solution.

The GPMT consists of an induction phase, in which animals are exposed to the test material through intradermal and topical applications, followed by a challenge exposure after a resting period to determine whether a delayed hypersensitivity reaction develops. Guinea pigs were shaved dorsally, and 0.1 mL of the BC/GSO extract was injected intradermally in the interscapular region. Seven days later, the BC/GSO dressing was applied topically to the same region and secured with gauze and mesh for 48 h. Fourteen days after this topical induction, a challenge exposure was performed by applying the BC/GSO dressing topically to the interscapular region for 24 h. Skin reactions were evaluated 24 and 48 h after patch removal according to the Magnusson and Kligman grading scale [67], where scores ≥ 1 in at least 30% of the test group are considered indicative of sensitization.

2.2.8. Healing Test

The healing test was performed on Wistar laboratory rats (live body weight of 143–150 g) with diabetes induced by intraperitoneal administration of streptozotocin. The test was initiated once the experimental model was confirmed by fasting glucose values above 180 mg/dL. The protocol for the use of animals was approved by the Internal Committee for the Care of Laboratory Animals of CIATEJ, A.C.

Twelve diabetic rats were randomly allocated into three groups of four animals each: a treatment group receiving BC/GSO 1:500 (v/v) dressings, a reference group treated with nitrofurazone (Furacin®, 2 mg/g), and an untreated control group. After confirmation of diabetes, the dorsal region of the rats was shaved and disinfected with a sterile antiseptic solution. Under anesthesia, a full-thickness excisional wound approximately 2 cm in length was created using a sterile surgical scalpel. Wound healing progression was monitored by measuring wound length at predetermined time intervals using a digital vernier caliper, and the general health condition of the animals was monitored throughout the experimental period. Wound length measurements were performed by the same operator throughout the study; blinding of the assessor was therefore not implemented. Wound contraction (%) was calculated using Equation (1):

$$\text{Wound contraction } (\%) = \frac{L_0 - L_t}{L_0} \times 100 \quad (1)$$

where L_0 represents the initial wound length (approximately 2 cm) and L_t corresponds to the wound length at time t. Data are reported as group means; no inferential statistical analysis was performed.

3. Results

Bacterial cellulose (BC) membranes were produced from mango pulp agro-waste (MPW) and subsequently functionalized with grapefruit seed oil (GSO). The biological performance of BC/GSO membranes was evaluated through in vivo and in vitro assays. These analyses included antimicrobial activity against representative microorganisms, cytotoxicity and mutagenicity assessments, pyrogenicity and sensitization tests, and an in vivo wound healing study using a diabetic rat model.

3.1. Production of BC from Mango Pulp Agro-Waste (MPW)

The production of BC by *K. xylinus* DSM 2004 was evaluated in MPW-based and HS culture media under static conditions. After 16 days of incubation, the BC yield obtained in the MPW medium was 6.32 g/L, compared to 1.94 g/L in the HS control. The membranes formed at the air-liquid interface and reached a thickness of approximately 2 mm in the hydrated state under the cultivation conditions used (20 mL of medium in 10 cm-diameter glass containers). Representative images of the purified hydrated membrane and the freeze-dried membrane are shown in Figures 2A and 2B, respectively.

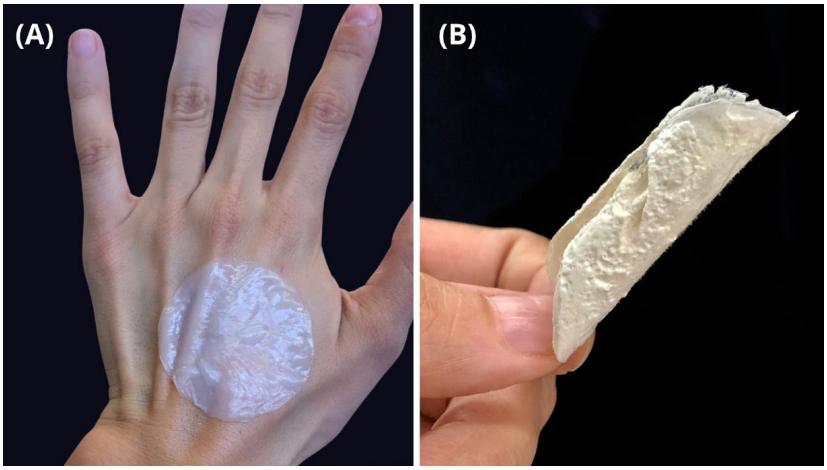


Figure 2. Bacterial cellulose membranes produced from mango pulp agro-waste (MPW). (**A**) Hydrated, purified BC membrane after 16 days of static cultivation. (**B**) Freeze-dried BC membrane.

The main physicochemical properties of the BC membranes obtained in both media are summarized in Table 1, with values reported in our previous work [60]. MPW-derived BC showed a higher yield, higher water holding capacity and smaller fiber diameter, with a lower crystallinity index. The thermal degradation behavior was similar in both media, with onset values between 340 and 360 °C, indicating that the use of MPW does not affect the thermal stability of the polymer.

Table 1. Physicochemical properties of bacterial cellulose membranes produced by *K. xylinus* DSM 2004 in mango pulp agro-waste (MPW)-based and HS culture media. Values from [60].

Property	MPW-Based Medium	HS Medium (Control)
BC yield (g/L)	6.32	1.94
$Y_{P/S}$ (g BC/g substrate consumed)	0.09	0.046
Water holding capacity (g water/g dry BC)	108.7	88.7
Average nanofiber diameter (nm)	50.6	98.8
Crystallinity index (%)	62.7	77.2
Thermal degradation onset (°C)	340–360	340–360
Membrane thickness, hydrated state (mm)	~2	~2

The lower crystallinity of MPW-derived BC has been associated with the presence of pectin and other polymeric compounds in mango pulp that interfere with microfibril aggregation during biosynthesis [60]. For wound dressing applications, this lower crystallinity is favorable, as it improves water uptake and permeability to functional substances. Together with the higher yield and the use of an agro-industrial residue as a carbon source, these results support the use of MPW as a sustainable alternative to conventional HS medium to produce biomedical-grade BC [14,15].

3.2. FTIR Analysis of BC/GSO Membranes

The incorporation of GSO into BC membranes was evaluated by FTIR spectroscopy. The spectra of pure BC, pure GSO and the BC/GSO functionalized membranes are shown in Figure 3. The spectrum of BC showed the characteristic bands of cellulose, including the broad O-H stretching near 3340 cm^{-1}, the C-H stretching of the glucopyranose ring close to 2900 cm^{-1}, and the C-O-C asymmetric stretching of the β-(1,4) glycosidic linkage in the 1000–1100 cm^{-1} region [60]. The spectrum of pure GSO showed sharp absorption bands in the regions typically associated with the aliphatic C-H stretching (2900–2850 cm^{-1}) and the C=C stretching of citrus terpene compounds, in agreement with profiles reported for grapefruit seed oil and other citrus oil-based formulations [68,69].

The BC/GSO membranes showed a concentration-dependent incorporation of GSO. The aliphatic C-H doublet at 2920/2855 cm^{-1}, associated with the aliphatic chains of GSO and not observed in pristine BC, appeared in all functionalized samples and increased in intensity from BC/GSO 1:500 to 1:100 (*v*/*v*). The main cellulose bands were preserved across all samples, indicating that the structure of the BC matrix was not modified by the functionalization process, suggesting that GSO incorporation occurs predominantly through capillary absorption and non-covalent interactions within the nanofibrillar network [68].

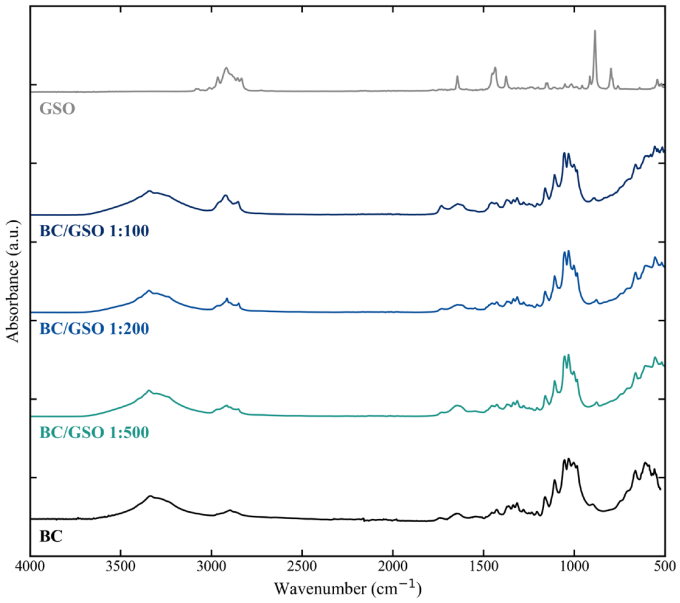


Figure 3. FTIR-ATR spectra of bacterial cellulose (BC), grapefruit seed oil (GSO), and BC/GSO membranes at 1:500, 1:200, 1:100 (*v*/*v*) ratios.

3.3. Antimicrobial Activity of Functionalized BC/GSO Dressings

BC membranes functionalized with grapefruit seed oil (GSO) exhibited antimicrobial activity against the three evaluated microorganisms. Representative agar plates showing the inhibition radii observed for each microorganism and treatment are presented in Figure 4. The comparative inhibition radii against the three microorganisms are shown in Figure 5, with the corresponding numerical values provided in Table S1 (Supplementary Materials). No inhibition zones were observed for the non-functionalized BC membranes used as the negative control, confirming that BC itself does not exhibit antimicrobial activity. The positive control (gentamicin, 10 µg/disc) produced clear inhibition zones in all three strains, validating the assay conditions.

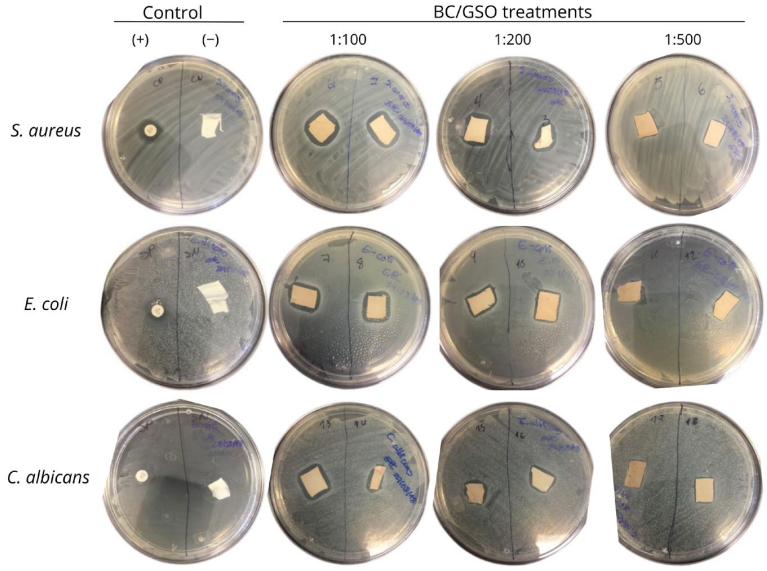


Figure 4. Representative agar plates showing the antimicrobial activity of bacterial cellulose (BC) membranes functionalized with grapefruit seed oil (GSO) against *Staphylococcus aureus*, *Escherichia coli*, and *Candida albicans*. The positive control (+) corresponds to gentamicin (10 µg/disc), while the negative control (−) corresponds to non-functionalized BC membranes. Different GSO dilutions (1:100, 1:200 and 1:500 *v*/*v*) were evaluated.

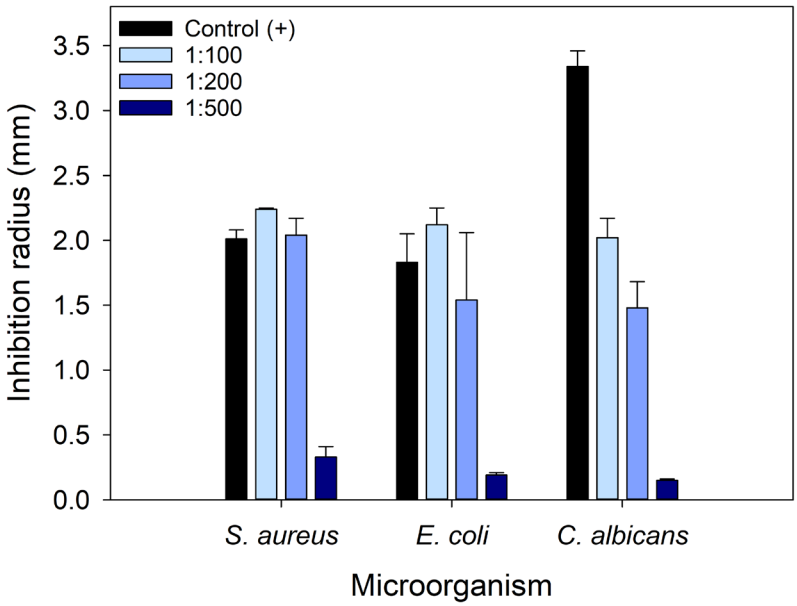


Figure 5. Inhibition radii (mm) of BC/GSO membranes against *Staphylococcus aureus*, *Escherichia coli*, and *Candida albicans*. The positive control (+) corresponds to gentamicin (10 μg/disc). Different GSO dilutions (1:100, 1:200, and 1:500 *v*/*v*) are shown for comparison.

The antimicrobial activity of the BC/GSO membranes was concentration-dependent. The most concentrated formulation (BC/GSO 1:100 *v*/*v*) produced the largest inhibition zones, comparable to gentamicin, followed by 1:200 (*v*/*v*), with a marked reduction in activity at 1:500 (*v*/*v*). This trend was consistent across *Staphylococcus aureus*, *Escherichia coli*, and *Candida albicans*, indicating that the antimicrobial effect of GSO-functionalized BC membranes is maintained across Gram-positive, Gram-negative, and yeast strains, a typical behavior of essential oils [54].

Although the BC/GSO 1:100 (*v*/*v*) formulation showed the highest antimicrobial activity, the BC/GSO 1:500 (*v*/*v*) formulation was selected for the subsequent biocompatibility and in vivo evaluations as the minimum effective dose that retained measurable antimicrobial activity, in line with the minimal effective dose principle commonly applied in preclinical evaluation of medical devices.

3.4. Cytotoxicity and Mutagenicity

The cytotoxicity of the BC/GSO 1:500 (*v*/*v*) dressings was evaluated by the MTT assay in NIH/3T3 fibroblast cells. Cell viability results are presented in Figure 6. The untreated cell control was considered as 100% viability. The positive control, cisplatin (cis-diamminedichloroplatinum, 12.5–200 μg/mL), exhibited a dose-dependent decrease in cell viability, confirming the reliability of the assay.

The BC/GSO 1:500 (*v*/*v*) extract was evaluated through serial 10-fold dilutions in endotoxin-free water (1:1000 to 1:1,000,000), and cell viability showed a clear concentration-dependent response. Lower dilutions (higher extract concentrations), such as 1:1000, resulted in reduced cell viability (around 14%), indicating a cytotoxic effect at high concentrations. At 1:10,000, viability remained close to the 70% threshold required by ISO 10993-5:2009 [63], while at dilutions of 1:100,000 or higher, it consistently exceeded the threshold, reaching values above 80% at 1:100,000 and 94% at 1:1,000,000.

Following the threshold established by ISO 10993-5:2009 [63], BC/GSO 1:500 (*v*/*v*) extracts were considered non-cytotoxic from dilution 1:100,000 onwards. The MTT assay was performed as a single experiment without replicates, as described in Section 2.2.5.

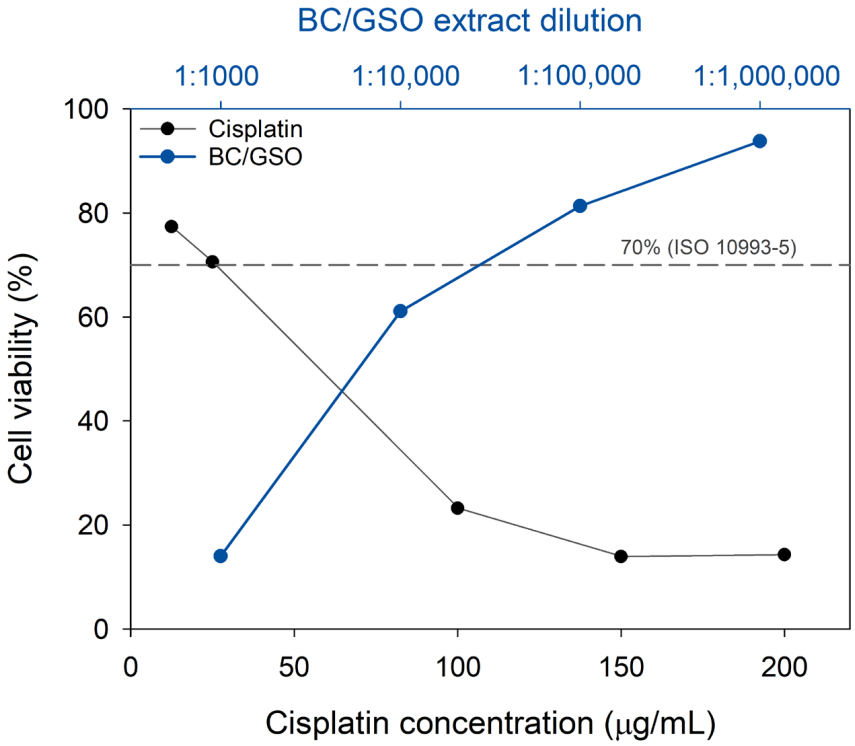


Figure 6. Cell viability (%) of NIH/3T3 fibroblasts exposed to cisplatin and BC/GSO extracts. Cisplatin concentrations are shown on the bottom *x*-axis, while BC/GSO 1:500 (*v*/*v*) extract dilutions are shown on the top *x*-axis. The dashed horizontal line indicates the non-cytotoxicity threshold (70%, ISO 10993-5:2019 [63]).

The mutagenicity results are presented in Table 2. The assay was considered valid, as the positive control (methyl methanesulfonate, MMS) produced a significant increase in the number of revertant colonies compared to the negative control, confirming the sensitivity of the test system.

Table 2. Mutagenicity assessment of BC/GSO 1:500 (*v*/*v*) dressings using the Ames test (*Salmonella typhimurium* TA100). Values are expressed as mean ± standard deviation (*n* = 3).

Sample	Revertant Colonies (Mean ± SD)	Mutagenicity
Negative control	75 ± 2.6	Negative
BC/GSO 1:500 (*v*/*v*)	73 ± 6.0	Negative
Positive control (MMS)	268 ± 11.5	Positive

The BC/GSO 1:500 (*v*/*v*) extracts showed an average of 73 ± 6.0 revertant colonies per plate, which is comparable to the negative control (75 ± 2.6) and well below the response observed for the positive control (268 ± 11.5). This indicates that the BC/GSO 1:500 (*v*/*v*) dressings did not induce a mutagenic response in the *Salmonella typhimurium* strain TA100.

3.5. Pyrogenicity Test

The pyrogenicity of BC/GSO 1:500 (*v*/*v*) dressings was evaluated using the rabbit pyrogen test by measuring temperature changes (ΔT) relative to baseline. The body temperature profiles of the rabbits during the pyrogenicity test are summarized in Table 3, and the corresponding ΔT values are shown in Figure 7.

Table 3. Body temperature (°C) of rabbits during the pyrogenicity test of BC/GSO 1:500 (*v*/*v*) dressings. Baseline values were recorded prior to sample administration.

Rabbit (Weight)	Body Temperature (°C)						
	Baseline	0.5 h	1.0 h	1.5 h	2.0 h	2.5 h	3.0 h
1 (2.90 kg)	39.3	38.9	38.5	38.3	38.7	38.5	38.7
2 (2.70 kg)	39.7	39.1	38.4	38.1	38.3	38.7	39.3
3 (2.95 kg)	39.7	39.5	38.6	38.4	37.2	38.5	38.1

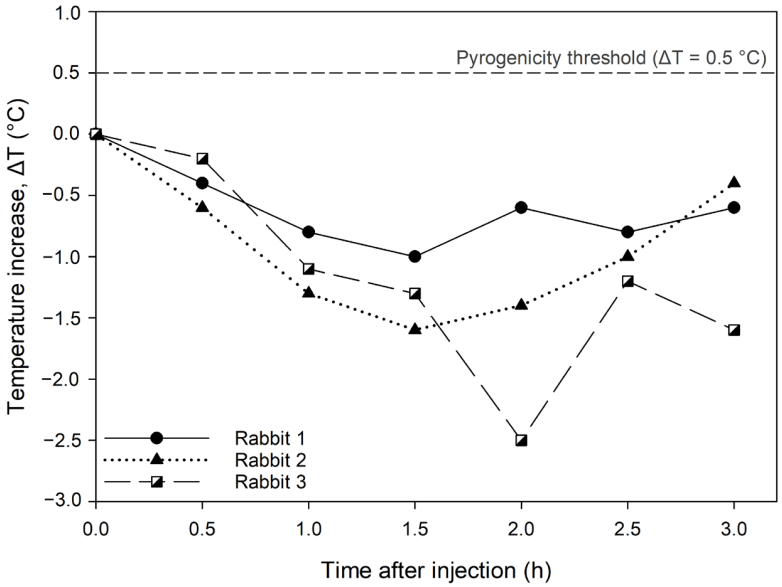


Figure 7. Temperature increase (ΔT, °C) of three rabbits during the pyrogenicity test of BC/GSO 1:500 (*v*/*v*) dressings. The dashed horizontal line indicates the pharmacopeial acceptance limit (0.5 °C above baseline [65]).

All three rabbits showed negative ΔT values at every time point recorded after sample administration, indicating that body temperature remained below the pre-injection baseline throughout the 3 h observation period. None of the recorded values approached or exceeded the pharmacopeial acceptance limit of 0.5 °C above baseline. Minor temperature fluctuations observed across the observation period remained within the range of normal physiological variability in rabbit body temperature and at no point exceeded the pre-injection baseline. These results indicate that the BC/GSO 1:500 (*v*/*v*) dressings are non-pyrogenic under the tested conditions.

3.6. Sensitization Test

The sensitization potential of the BC/GSO 1:500 (*v*/*v*) dressings was evaluated using the Guinea Pig Maximization Test (GPMT) following the Magnusson and Kligman grading scale [67]. Skin reactions were assessed at 24 and 48 h after the challenge phase, and the results are summarized in Table 4.

None of the animals in the treatment group exhibited any visible signs of skin sensitization at either evaluation time point. All scores were recorded as 0, corresponding to the absence of erythema or edema according to the Magnusson and Kligman scale. The control group, treated with non-functionalized BC membranes, also showed no observable skin reactions at either time point, confirming that the BC matrix itself does not induce hypersensitivity under the tested conditions. These results indicate that the BC/GSO 1:500 (*v*/*v*) dressings did not induce delayed hypersensitivity reactions under the tested conditions.

Table 4. Skin sensitization scores of BC/GSO 1:500 (*v*/*v*) dressings (treatment) and non-functionalized BC membranes (control) evaluated by the Guinea Pig Maximization Test (GPMT) at 24 and 48 h after challenge exposure. Scores were assigned according to the Magnusson and Kligman scale (0–3), where 0 indicates no visible reaction, and 3 indicates severe erythema and/or edema.

Group	Animal	24 h	48 h
Treatment	1	0	0
	2	0	0
	3	0	0
	4	0	0
	5	0	0
	6	0	0
	7	0	0
	8	0	0
	9	0	0
	10	0	0
Control	11	0	0
	12	0	0
	13	0	0
	14	0	0
	15	0	0

3.7. Healing Test

The wound healing process was evaluated by monitoring wound length reduction and calculating the percentage of wound contraction over a 21-day period. Wound length values are summarized in Table 5, and the corresponding wound contraction profiles over time are shown in Figure 8. All groups exhibited an initial wound length of approximately 2 cm at day 0, and differences in healing progression became evident over time among the experimental groups.

Table 5. Wound length (cm) over time for untreated control, nitrofurazone-treated, and BC/GSO 1:500 (*v*/*v*) dressing groups. Data are presented as mean ± SD ($n = 4$).

Time (Days)	Wound Length (cm)		
	Control	Nitrofurazone	BC/GSO 1:500 (*v*/*v*) Dressing
0	2.0 ± 0.0	2.0 ± 0.0	2.0 ± 0.0
7	2.0 ± 0.0	1.5 ± 0.0	1.6 ± 0.3
14	2.0 ± 0.0	1.5 ± 0.0	1.6 ± 0.3
21	1.5 ± 0.0	1.0 ± 0.0	1.1 ± 0.3

As observed, by day 21, BC/GSO 1:500 (*v*/*v*) reached 43.8 ± 12.5% wound contraction, comparable to nitrofurazone (50.0 ± 0.0%) and higher than the untreated control (25.0 ± 0.0%). Between days 7 and 14, no further reduction in wound length was observed in any of the three groups, suggesting a transient plateau in the contraction process consistent with the delayed healing dynamics typically reported in streptozotocin-induced diabetic models [70]. Both the BC/GSO 1:500 (*v*/*v*) dressing and nitrofurazone treatments promoted wound closure compared to the untreated control. The BC/GSO 1:500 (*v*/*v*) group showed wound contraction comparable to nitrofurazone, with higher inter-individual variability that reflects the limited sample size ($n = 4$). No clinical signs of wound infection were observed in any of the three groups during the 21-day follow-up period. Complementary qualitative macroscopic evaluation of healing progression is provided in Figure S2 (Supplementary Materials).

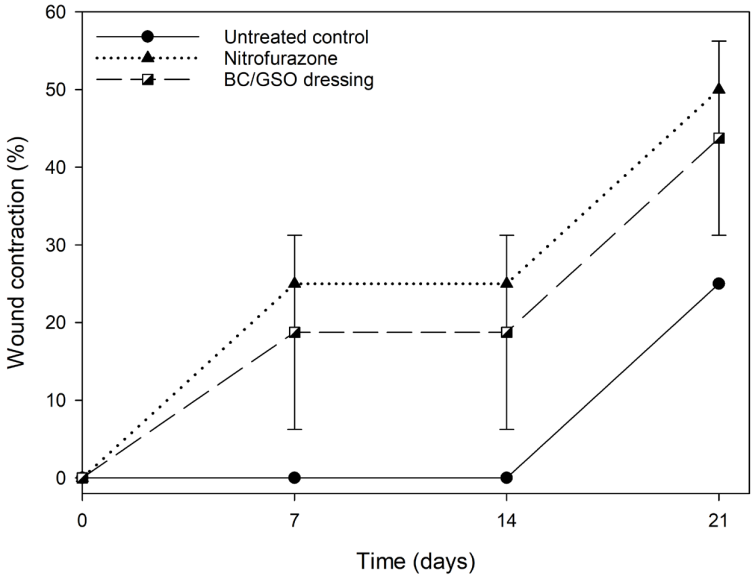


Figure 8. Wound contraction (%) over time in untreated control, nitrofurazone-treated and BC/GSO 1:500 (*v*/*v*) dressing groups. Data are presented as mean ± SD (*n* = 4).

4. Discussion

The use of mango pulp agro-waste as a carbon source for *K. xylinus* cultivation provides a low-cost alternative to conventional synthetic media such as Hestrin–Schramm, whose high cost has long limited the industrial scale-up of bacterial cellulose production [17]. Beyond cost reduction, mango pulp agro-waste also outperformed HS in BC yield (6.32 vs. 1.94 g/L), water-holding capacity and fiber diameter, confirming that nutrient-rich agro-industrial residues can match or exceed the performance of standardized media in BC biosynthesis [60,71]. The strategy is consistent with the broader trend of valorizing fruit-processing residues into biomedical-grade biopolymers, contributing to the circular economy framework while reducing the environmental footprint of BC manufacturing [17].

The FTIR analysis of the BC/GSO membranes confirmed that GSO incorporation into the BC matrix occurred predominantly through physical interactions, in agreement with previous studies on the incorporation of citrus-derived oils and other essential oils in polysaccharide-based films [68,69]. The intensity of the aliphatic C-H bands of GSO increased progressively from BC/GSO 1:500 to 1:100 (*v*/*v*), revealing a dose-dependent loading consistent with the impregnation mechanism described for similar systems. While this approach does not generate covalent bonds between GSO and BC, it offers a simple and scalable functionalization strategy compatible with biomedical-grade dressings [65]. A quantitative determination of GSO loading and a controlled in vitro release profile were not addressed in the present work and remain to be characterized in future studies.

The BC/GSO membranes showed antimicrobial activity against *Staphylococcus aureus*, *Escherichia coli*, and *Candida albicans*, with inhibition zones increasing from BC/GSO 1:500 to BC/GSO 1:100 (*v*/*v*). This concentration-dependent behavior is in line with the dose–response patterns commonly reported for citrus and other plant-derived essential oils incorporated in polysaccharide matrices, where antimicrobial activity scales with the amount of active compound [69,72]. A common challenge in this class of materials is to identify the lowest active concentration that retains antimicrobial efficacy while preserving cytocompatibility, since highly loaded formulations often compromise cell viability.

The need to balance antimicrobial activity with cell viability has been documented in different dressing systems, including silver nanoparticle-functionalized cotton gauzes, where the lowest silver-precursor concentration tested (0.5% *w*/*w*) was selected as the optimal balance between antimicrobial activity, biocompatibility and material economy [73],

as well as in polymer-based dressings loaded with plant-derived essential oils, where dose selection follows the same principle [74].

In this sense, the BC/GSO 1:500 (*v*/*v*) dressing was selected for the subsequent biocompatibility and in vivo evaluations as the minimum effective dose retaining measurable antimicrobial activity. This selection was further supported by the overall biocompatibility profile of the BC/GSO 1:500 (*v*/*v*) formulation, which met the cytotoxicity threshold established by ISO 10993-5:2009 [63] and showed no mutagenic, pyrogenic or sensitizing responses, together with effective wound closure under diabetic conditions in vivo. The biocompatibility/in vivo characterization of the more concentrated formulations (1:100 and 1:200 *v*/*v*) was not addressed in the present work, also consistent with the 3Rs principle (Replacement, Reduction, Refinement) of minimizing the use of animals in preclinical research [75].

The biocompatibility of the BC/GSO 1:500 (*v*/*v*) dressings was evaluated through a multi-test panel (cytotoxicity, mutagenicity, pyrogenicity and sensitization) following ISO 10993-1:2018 standards [76]. Cell viability increased with extract dilution and exceeded the 70% threshold established by ISO 10993-5:2009 [63] from 1:100,000 onwards, reaching 94% at 1:1,000,000. The reduced viability observed at lower dilutions is consistent with the dose-dependent cytotoxicity commonly reported for essential oils, attributed to their lipophilic terpene constituents and their interaction with cell membranes at high concentrations [77]. Similar trends, where polymer-based dressings loaded with essential oils only meet cytocompatibility criteria after dilution, have been reported in different polymer/essential oil systems [74]. The values obtained for BC/GSO 1:500 (*v*/*v*) are comparable to those reported by Qiu et al. [78], who observed cell growth around 74% for BC and BC-vaccarin functionalized membranes.

Cytotoxicity testing was performed on aqueous extracts of the membranes (ISO 10993-12:2021 [62]), rather than through direct contact with the material, representing the actual exposure of cells to substances released from the dressing under clinical use. The MTT assay was conducted as a single experiment without replicates, which constitutes a limitation of the present study; nevertheless, the consistent dose–response across four dilution orders supports the cytocompatibility of the BC/GSO 1:500 (*v*/*v*) formulation above the regulatory threshold.

The BC/GSO 1:500 (*v*/*v*) dressings also showed no mutagenic activity in the Ames test against *Salmonella typhimurium* TA100, indicating that the bioactive compounds released from the matrix did not produce genotoxic responses under the tested conditions. The pyrogenicity test confirmed that the BC/GSO 1:500 (*v*/*v*) dressings do not induce febrile responses, as none of the evaluated subjects exhibited temperature increases equal to or greater than 0.5 °C. These results are in line with previous studies on BC-based systems. Kołaczkowska et al. [79] reported that BC implants did not exhibit pyrogenic responses, remaining below the limits established by the Polish and European Pharmacopoeias [80]. Similarly, Szymanski et al. [81] demonstrated that polysaccharide-based materials, including BC, do not induce significant temperature increases, reinforcing the intrinsic biocompatibility of this class of biomaterials.

Finally, the GPMT confirmed the absence of delayed hypersensitivity, with all sensitization scores recorded as zero in both BC/GSO 1:500 (*v*/*v*) and non-functionalized BC control groups, indicating that neither the matrix nor the GSO load elicited a sensitizing response. This outcome is particularly relevant given that essential oils have been reported to cause dermal sensitization at high concentrations [74], reinforcing the rationale for selecting the 1:500 (*v*/*v*) formulation. Together with the cytotoxicity, mutagenicity and pyrogenicity results, the absence of sensitization completes the biocompatibility profile required by ISO 10993-1:2018 [76] for medical devices in prolonged skin contact.

The in vivo wound healing results further support the functional performance of BC/GSO 1:500 (*v*/*v*) dressings under diabetic conditions. Both BC/GSO and nitrofurazone-treated groups exhibited a clear reduction in wound length compared to the untreated control, with final wound contractions of 43.8 ± 12.5% and 50.0 ± 0.0%, respectively, against 25.0 ± 0.0% in the control group. The BC/GSO dressing reached a healing performance comparable to nitrofurazone, supporting its potential as an alternative wound-care option. Between days 7 and 14, no further reduction in wound length was observed in any of the three groups, suggesting a transient plateau in the healing dynamics. This behavior is consistent with the delayed wound healing reported for streptozotocin-induced diabetic models, where impaired re-epithelialization, reduced angiogenesis and slower closure rates have been documented during the intermediate stages of the healing process [70].

The ability of BC-based materials to maintain a moist environment, combined with their structural compatibility and bioactivity, plays a crucial role in promoting effective tissue repair [82]. The wound healing performance observed in this study, together with the absence of clinical signs of infection during the 21-day follow-up, supports the use of GSO as a safe functionalization strategy for BC-based dressings. These outcomes also indicate that the antimicrobial activity retained at the 1:500 (*v*/*v*) concentration was sufficient to prevent wound infection under in vivo conditions, complementing the biocompatibility results obtained in vitro. It should be acknowledged that the in vivo evaluation was based on a limited sample size ($n = 4$) without inferential statistical analysis, and was restricted to wound length measurements. Histological evaluation, wound area quantification and molecular markers of inflammation and angiogenesis are identified as future research directions.

Overall, BC/GSO 1:500 (*v*/*v*) dressings produced from mango pulp agro-waste combine antimicrobial activity, biocompatibility and effective wound closure under diabetic conditions, supporting their preclinical viability as a functional dressing for diabetic wound care.

5. Conclusions

This study reports the development and preclinical evaluation of bacterial cellulose membranes produced from mango pulp agro-waste and functionalized with grapefruit seed oil for diabetic wound dressing applications. The combined assessment of antimicrobial activity, biocompatibility (cytotoxicity, mutagenicity, pyrogenicity and sensitization) and in vivo wound healing under diabetic conditions supports the preclinical viability of BC/GSO 1:500 (*v*/*v*) dressings as a functional material for early-stage development in diabetic wound care.

The functionalization of BC with GSO at a 1:500 (*v*/*v*) ratio retained measurable antimicrobial activity against *Staphylococcus aureus*, *Escherichia coli* and *Candida albicans*, while meeting the cytotoxicity threshold defined by ISO 10993-5:2009 [63] and showing no mutagenic, pyrogenic or sensitizing responses. In vivo, the BC/GSO 1:500 (*v*/*v*) dressings supported wound closure under diabetic conditions with a performance comparable to nitrofurazone and superior to the untreated control, with no clinical signs of infection during the follow-up period.

The biocompatibility evaluation, following the ISO 10993-1:2018 [76] standards, provides a regulatory-aligned dataset that supports the early-stage positioning of BC/GSO dressings as candidate biomaterials for skin contact and wound care applications. The application of the minimum effective dose principle in formulation selection further supports the suitability of the 1:500 (*v*/*v*) formulation for translational progression and process scale-up. The use of mango pulp agro-waste as a carbon source for *K. xylinus* cultivation provides a low-cost and environmentally favorable alternative to conventional synthetic media, contributing to the valorization of fruit-processing residues into biomedical-grade biopolymers in alignment with circular economy principles.

Future work should include the histological evaluation of the wound healing process, the quantification of wound area and the analysis of molecular markers of inflammation and angiogenesis. The quantitative determination of GSO loading and the characterization of in vitro release profiles, together with the mechanical and swelling properties of the dressings, are also identified as relevant directions in order to support the translational progression of BC/GSO dressings toward clinical evaluation.

Supplementary Materials: The following supporting information can be downloaded at: https://www.mdpi.com/article/10.3390/polysaccharides7020069/s1, Table S1. Inhibition radius (mm) of BC/GSO membranes against *Staphylococcus aureus*, *Escherichia coli*, and *Candida albicans*. Values are expressed as mean ± standard deviation (n = 3). Control (+): gentamicin (10 μg/disc); Control (−): non-functionalized BC membranes.; Figure S1. Representative images of the pyrogenicity test procedure performed on three New Zealand albino rabbits (*Oryctolagus cuniculus*) according to MGA Method 0711 of the Medical Device Supplement to the Mexican Pharmacopeia. (A) Rectal temperature measurement using a Welch Allyn SureTemp Plus electronic thermometer. (B) Aseptic preparation of the BC/GSO 1:500 (v/v) extract prior to administration. (C) Intravenous administration of the test extract through the marginal ear vein. Temperature was monitored at baseline and at 30 min intervals over 3 h. Figure S2. Representative macroscopic images of wound healing progression in streptozotocin-induced diabetic Wistar rats (n = 4 per group, initial wound size approximately 2 cm). (A,D,G) Untreated control group at days 7, 14, and 21, respectively. (B,E,H) Nitrofurazone-treated group at days 7, 14, and 21, respectively. (C,F,I) BC/GSO 1:500 (v/v) dressing group at days 7, 14, and 21, respectively. Images correspond to one representative animal per group at each time point and complement the quantitative analysis presented in Table 5 and Figure 8.

Author Contributions: Conceptualization, M.E.G.-S. and I.J.-P.; methodology, M.E.G.-S. and A.B.-C.; formal analysis, M.E.G.-S., A.B.-C., J.M.A.-C., I.J.-P. and E.O.C.-L.; investigation, M.E.G.-S., A.B.-C., J.M.A.-C., I.J.-P. and E.O.C.-L.; writing—original draft preparation, M.E.G.-S.; writing—review and editing, M.E.G.-S., J.M.A.-C., I.J.-P. and E.O.C.-L.; visualization, M.E.G.-S., I.J.-P. and E.O.C.-L.; supervision, I.J.-P. and E.O.C.-L.; project administration, I.J.-P.; funding adquisition, I.J.-P. and E.O.C.-L. Author A.B.-C. passed away prior to the publication of this manuscript. All other authors have read and agreed to the published version of the manuscript.

Funding: This research received no external funding.

Institutional Review Board Statement: The animal study protocols were reviewed and approved by the Internal Committee for the Care and Use of Laboratory Animals of CIATEJ, A.C. (CICUAL/CIATEJ) on 9 January 2019, under the following protocol codes: 2018-011 (pyrogenicity test and in vivo wound healing test), 2018-013 (sensitization test) and 2018-008 (skin irritation test). All procedures were conducted in accordance with NOM-062-ZOO-1999 [83] and ISO 10993-1:2018 [76] (Biological Evaluation of Medical Devices), and following MGA Method 0711 of the Medical Device Supplement to the Mexican Pharmacopeia (Fourth Edition) [65].

Informed Consent Statement: Not applicable.

Data Availability Statement: The data presented in this study are available from the corresponding author upon reasonable request.

Acknowledgments: The authors would like to express their sincere gratitude and dedicate this paper to the beloved memory of Alfonso Barajas Cervantes, M.S. For his invaluable technical support, his critical and objective evaluation of this research and his dedicated contribution. His experience and commitment left a significant mark on this project and on all who had the privilege of collaborating with him.

Conflicts of Interest: Authors Mayra Elizabeth García-Sánchez (M.E.G.-S.) and Inés Jiménez-Palomar (I.J.-P.) in the manuscript are affiliated with the company inMateriis S.A. de C.V., which may have a commercial interest in the materials discussed in this study. The remaining authors declare no conflicts of interest.

References

1. Seddiqi, H.; Oliaei, E.; Honarkar, H.; Jin, J.; Geonzon, L.C.; Bacabac, R.G.; Klein-Nulend, J. Cellulose and its derivatives: Towards biomedical applications. *Cellulose* **2021**, *28*, 1893–1931. [CrossRef]
2. Chen, Z.; Aziz, T.; Sun, H.; Ullah, A.; Ali, A.; Cheng, L.; Ullah, R.; Khan, F.U. Advances and applications of cellulose bio-composites in biodegradable materials. *J. Polym. Environ.* **2023**, *31*, 2273–2284. [CrossRef]
3. French, A.D. Increment in evolution of cellulose crystallinity analysis. *Cellulose* **2020**, *27*, 5445–5448. [CrossRef]
4. Akerholm, M.; Hinterstoisser, M.B.; Salmén, L. Characterization of the crystalline structure of cellulose using static and dynamic FT-IR spectroscopy. *Carbohydr. Res.* **2004**, *339*, 569–578. [CrossRef]
5. Gregory, D.A.; Tripathi, L.; Fricker, A.T.R.; Asare, E.; Orlando, I.; Raghavendran, V.; Roy, I. Bacterial cellulose: A smart biomaterial with diverse applications. *Mater. Sci. Eng. R Rep.* **2021**, *145*, 100623. [CrossRef]
6. Choi, S.M.; Rao, K.M.; Zo, S.M.; Shin, E.J.; Han, S.S. Bacterial cellulose and its applications. *Polymers* **2022**, *14*, 1080. [CrossRef]
7. Raiszadeh-Jahromi, Y.; Rezazadeh-Bari, M.; Almasi, H.; Amiri, S. Optimization of bacterial cellulose production by *Komagataeibacter xylinus* PTCC 1734 in a low-cost medium using optimal combined design. *J. Food Sci. Technol.* **2020**, *57*, 2524–2533. [CrossRef]
8. Li, W.; Huang, X.; Liu, H.; Lian, H.; Xu, B.; Zhang, W.; Zhong, C. Improvement in bacterial cellulose production by co-culturing *Bacillus cereus* and *Komagataeibacter xylinus*. *Carbohydr. Polym.* **2023**, *313*, 120892. [CrossRef]
9. Marič, L.; Cleenwerck, I.; Accetto, T.; Vandamme, P.; Trček, J. Description of *Komagataeibacter melaceti* sp. nov. and *Komagataeibacter melomenusus* sp. nov. isolated from apple cider vinegar. *Microorganisms* **2020**, *8*, 1178. [CrossRef]
10. Gunduz, G.; Erbas Kiziltas, E.; Kiziltas, A.; Gencer, A.; Aydemir, D.; Asik, N. Production of bacterial cellulose fibers in the presence of effective microorganism. *J. Nat. Fibers* **2018**, *16*, 567–575. [CrossRef]
11. Rodrigues, D.M.; da Silva, M.F.; Almeida, F.L.C.; de Mélo, A.H.F.; Forte, M.B.S.; Martín, C.; Goldbeck, R. A green approach to biomass residue valorization: Bacterial nanocellulose production from agro-industrial waste. *Biocatal. Agric. Biotechnol.* **2024**, *56*, 103036. [CrossRef]
12. Shrivastav, P.; Pramanik, S.; Vaidya, G.; Abdelgawad, M.A.; Ghoneim, M.M.; Singh, A.; Abualsoud, B.M.; Amaral, L.S.; Abourehab, M.A.S. Bacterial cellulose as a potential biopolymer in biomedical applications: A state-of-the-art review. *J. Mater. Chem. B* **2022**, *10*, 3199–3241. [CrossRef]
13. Gorgieva, S. Bacterial cellulose as a versatile platform for research and development of biomedical materials. *Processes* **2020**, *8*, 624. [CrossRef]
14. Jozala, A.F.; de Lencastre-Novaes, L.C.; Lopes, A.M.; Santos-Ebinuma, V.D.C.; Mazzola, P.G.; Pessoa, A., Jr.; Grotto, D.; Gerenutti, M.; Chaud, M.V. Bacterial nanocellulose production and application: A 10-year overview. *Appl. Microbiol. Biotechnol.* **2016**, *100*, 2063–2072. [CrossRef]
15. Meslier, T.; D'Antin, J.C.; Julio, G.; Roig, A. A Comprehensive Review of Clinical Studies on Bacterial Cellulose: From the Earliest Uses to Contemporary Innovations. *Adv. Healthc. Mater.* **2025**, *14*, e02189. [CrossRef]
16. Haslan, H.A.; Halim, M.; Rahman, N.A.; Sobri, Z.M.; Yusof, M.T.; Pak-Dek, M.S.; Wasoh, H. Integrated Factors Influencing Bacterial Cellulose Production in Kombucha SCOBY: Bioprocess Strategies for Enhanced Yield. *J. Biochem. Microbiol. Biotechnol.* **2025**, *13*, 70–76. [CrossRef]
17. Belkozhayev, A.M.; Abaildayev, A.; Kossalbayev, B.D.; Tastambek, K.T.; Kadirshe, D.K.; Toleutay, G. Microbial Valorization of Agricultural and Agro-Industrial Waste into Bacterial Cellulose: Innovations for Circular Bioeconomy Integration. *Microorganisms* **2025**, *13*, 2686. [CrossRef]
18. Catarino, R.P.F.; Mascareli, V.A.B.; Leite da Costa, V.L.; Pavanello, A.C.L.; Spinosa, W.A. Sustainability and Influencing Factors in Bacterial Cellulose Production: A Review of the Impact of Microorganisms, Culture Media and Cultivation Methods. *Food Technol. Biotechnol.* **2025**, *63*, 332–350. [CrossRef]
19. Narváez-García, A.; Blanco-Cornelio, C.V.; Canedo-López, Y.; Robles-Heredia, J.C. Uso de mango criollo (Anacardiaceae) como alternativa para elaborar productos alimenticios y biofertilizante en el Estado de Campeche. *Tend. Energ. Renov. Sust.* **2026**, *5*, 16–23. [CrossRef]
20. Klemm, D.; Schumann, D.; Udhardt, U.; Marsch, S. Bacterial synthesized cellulose—Artificial blood vessels for microsurgery. *Prog. Polym. Sci.* **2001**, *26*, 1561–1603. [CrossRef]
21. Lu, Y.; Mehling, M.; Huan, S.; Bai, L.; Rojas, O.J. Biofabrication with microbial cellulose: From bioadaptive designs to living materials. *Chem. Soc. Rev.* **2024**, *53*, 7363. [CrossRef]
22. Saleh, A.K.; Taha, T.H.; Alenezi, H.; El-Fakharany, E.M.; Alhudhaibi, A.M.; Albatli, S.A.; Mohamed, M.Y.A.; El-Gendia, H. Overview of bacterial cellulose: Biosynthesis strategies, functionalization and biomedical marketing. *Biochimie* **2026**, *244*, 7–28. [CrossRef]
23. Zhou, B.; Rayner, A.W.; Gregg, E.W.; Sheffer, K.E.; Carrillo-Larco, R.M.; Bennett, J.E.; Shaw, J.E.; Paciorek, C.J.; Singleton, R.K.; Pires, A.B.; et al. Worldwide trends in diabetes prevalence and treatment from 1990 to 2022: A pooled analysis of 1108 population-representative studies with 141 million Participants. *Lancet* **2024**, *404*, 2077–2093. [CrossRef]

24. Banday, M.Z.; Sameer, A.S.; Nissar, S. Pathophysiology of diabetes: An overview. *Avicenna J. Med.* **2020**, *10*, 174–188. [CrossRef]
25. Rousselle, P.; Braye, F.; Dayan, G. Re-epithelialization of adult skin wounds: Cellular mechanisms and therapeutic strategies. *Adv. Drug Deliv. Rev.* **2019**, *146*, 344–365. [CrossRef]
26. Deng, H.; Li, B.; Shen, Q.; Zhang, C.; Kuang, L.; Chen, R.; Li, G. Mechanisms of diabetic foot ulceration: A review. *J. Diabetes* **2023**, *15*, 299–312. [CrossRef]
27. Caruso, I.; Leonardini, A.; Caizzi, G.; Vicenti, G.; Caporusso, M.; Guarini, F.; Bernardis, M.; Moretti, B.; Giorgino, F. Diabetic foot: Clinical approach. *Minerva Orthop.* **2022**, *73*, 63–75. [CrossRef]
28. Rubio, J.A.; Jiménez, S.; Lázaro-Martínez, J.L. Mortality in Patients with Diabetic Foot Ulcers: Causes, Risk Factors, and Their Association with Evolution and Severity of Ulcer. *J. Clin. Med.* **2020**, *9*, 3009. [CrossRef]
29. Chin, B.Z.; Lee, P.; Sia, C.H.; Hong, C.C. Diabetic foot ulcer is associated with cardiovascular-related mortality and morbidity—A systematic review and meta-analysis of 8062 patients. *Endocrine* **2024**, *84*, 852–863. [CrossRef]
30. de Amorim, J.D.P.; da Silva Junior, C.J.G.; de Medeiros, A.D.L.M.; do Nascimento, H.A.; Sarubbo, M.; de Medeiros, T.P.M.; Sarubbo, L.A. Bacterial cellulose as a versatile biomaterial for wound dressing application. *Molecules* **2022**, *27*, 5580. [CrossRef]
31. Falbo, F.; Spizzirri, U.G.; Restuccia, D.; Aiello, F. Natural Compounds and Biopolymers-Based Hydrogels Join Forces to Promote Wound Healing. *Pharmaceutics* **2023**, *15*, 271. [CrossRef]
32. Kolimi, P.; Narala, S.; Nyavanandi, D.; Youssef, A.A.A.; Dudhipala, N. Innovative treatment strategies to accelerate wound healing: Trajectory and recent advancements. *Cells* **2022**, *11*, 2439. [CrossRef]
33. Gomes, A.; Coelho, P.; Soares, R.; Costa, R. Human umbilical cord mesenchymal stem cells in type 2 diabetes mellitus: The emerging therapeutic approach. *Cell Tissue Res.* **2021**, *385*, 497–518. [CrossRef]
34. Momin, M.; Mishra, V.; Gharat, S.; Omri, A. Recent advancements in cellulose-based biomaterials for management of infected wounds. *Expert Opin. Drug Deliv.* **2021**, *18*, 1741–1760. [CrossRef]
35. Torgbo, S.; Sukyai, P. Biodegradation and thermal stability of bacterial cellulose as biomaterial: The relevance in biomedical applications. *Polym. Degrad. Stab.* **2020**, *179*, 109232. [CrossRef]
36. Mensah, A.; Chen, Y.; Asinyo, B.K.; Howard, E.K.; Narh, C.; Huang, J.; Wei, Q. Bioactive Icariin/β-CD-IC/Bacterial cellulose with enhanced biomedical potential. *Nanomaterials* **2021**, *11*, 387. [CrossRef]
37. Moniri, M.; Boroumand Moghaddam, A.; Azizi, S.; Abdul Rahim, R.; Bin Ariff, A.; Zuhainis Saad, W.; Navaderi, M.; Mohamad, R. Production and status of bacterial cellulose in biomedical engineering. *Nanomaterials* **2017**, *7*, 257. [CrossRef]
38. Alberts, A.; Tudorache, D.-I.; Niculescu, A.-G.; Grumezescu, A.M. Advancements in Wound Dressing Materials: Highlighting Recent Progress in Hydrogels, Foams, and Antimicrobial Dressings. *Gels* **2025**, *11*, 123. [CrossRef]
39. Tran, H.Q.; Shahriar, S.M.S.; Yan, Z.; Xie, J. Recent advances in functional wound dressings. *Adv. Wound Care* **2023**, *12*, 399–427. [CrossRef]
40. Rastogi, A.; Singh, J.; Das, M.; Kundu, D.; Banerjee, R. An understanding of bacterial cellulose and its potential impact on industrial applications. In *Principles and Applications of Fermentation Technology*; Elsevier: London, UK, 2018; pp. 437–458.
41. Yassue-Cordeiro, P.H.; Severino, P.; Souto, E.M.; Yoshida, C.M.P.; da Silva, C.F. Natural polysaccharides in wound dressing applications. In *Natural Polysaccharides in Drug Delivery and Biomedical Applications*; Academic Press: San Diego, CA, USA, 2019; pp. 549–566.
42. He, W.; Wu, J.; Xu, J.; Mosselhy, D.A.; Zheng, Y.; Yang, S. Bacterial cellulose: Functional modification and wound healing applications. *Adv. Wound Care* **2021**, *10*, 623–640. [CrossRef]
43. Horue, M.; Silva, J.M.; Berti, I.R.; Brandão, L.R.; Barud, H.d.S.; Castro, G.R. Bacterial Cellulose-Based Materials as Dressings for Wound Healing. *Pharmaceutics* **2023**, *15*, 424. [CrossRef]
44. Bianchet, R.T.; Cubas, A.L.V.; Machado, M.M.; Moecke, E.H.S. Applicability of bacterial cellulose in cosmetics—Bibliometric review. *Biotechnol. Rep.* **2020**, *27*, e00502. [CrossRef]
45. Dydak, K.; Junka, A.; Dydak, A.; Brożyna, M.; Paleczny, J.; Fijalkowski, K.; Kubielas, G.; Aniołek, O.; Bartoszewicz, M. In Vitro Efficacy of Bacterial Cellulose Dressings Chemisorbed with Antiseptics against Biofilm Formed by Pathogens Isolated from Chronic Wounds. *Int. J. Mol. Sci.* **2021**, *22*, 3996. [CrossRef]
46. Luzi, F.; Puglia, D.; Torre, L. Natural fiber biodegradable composites and nanocomposites: A biomedical application. In *Biomass, Biopolymer-Based Materials, and Bioenergy*, 1st ed.; Verma, D., Fortunati, E., Jain, S., Zhang, X., Eds.; Woodhead Publishing: Sawston, UK, 2019; Volume 1, pp. 179–201.
47. Sulaeva, I.; Henniges, U.; Rosenau, T.; Potthast, A. Bacterial cellulose as a material for wound treatment: Properties and modifications. A review. *Biotechnol. Adv.* **2015**, *33*, 1547–1571. [CrossRef]
48. Vivcharenko, V.; Trzaskowska, M.; Przekora, A. Wound Dressing Modifications for Accelerated Healing of Infected Wounds. *Int. J. Mol. Sci.* **2023**, *24*, 7193. [CrossRef]
49. Deng, X.; Gould, M.; Ali, M.A. A review of current advancements for wound healing: Biomaterial applications and medical devices. *J. Biomed. Mater. Res. B Appl. Biomater.* **2022**, *110*, 2542–2573. [CrossRef]

50. Choi, Y.S.; Lee, J.S.; Lee, H.G. Nanoencapsulation of grapefruit seed extract and cinnamon oil for oral health: Preparation, in vitro, and clinical antimicrobial activities. *J. Agric. Food Chem.* **2023**, *71*, 5646–5654. [CrossRef]
51. Zheng, Y.; Ley, S.H.; Hu, F.B. Global aetiology and epidemiology of type 2 diabetes mellitus and its complications. *Nat. Rev. Endocrinol.* **2018**, *14*, 88–98. [CrossRef]
52. de Sousa, D.P.; Damasceno, R.O.S.; Amorati, R.; Elshabrawy, H.A.; de Castro, R.D.; Bezerra, D.P.; Nunes, V.R.V.; Gomes, R.C.; Lima, T.C. Essential oils: Chemistry and pharmacological activities. *Biomolecules* **2023**, *13*, 1144. [CrossRef]
53. Logvina, Y.; Fernandes, S.; da Silva, L.P.; da Silva, J.E. Sustainable Sawdust/Eucalyptol Absorption Matrix for Odor Slow-Release in Plywood Floor. *Sustain. Chem.* **2023**, *4*, 236–245. [CrossRef]
54. Wińska, K.; Mączka, W.; Łyczko, J.; Grabarczyk, M.; Czubaszek, A.; Szumny, A. Essential Oils as Antimicrobial Agents—Myth or Real Alternative? *Molecules* **2019**, *24*, 2130. [CrossRef]
55. Hussain, Z.; Thu, H.E.; Shuid, A.N.; Katas, H.; Hussain, F. Recent advances in polymer-based wound dressings for the treatment of diabetic foot ulcer: An overview of state-of-the-art. *Curr. Drug Targets* **2018**, *19*, 527–550. [CrossRef]
56. Deng, W.; Liu, K.; Cao, S.; Sun, J.; Zhong, B.; Chun, J. Chemical composition, antimicrobial, antioxidant, and antiproliferative properties of grapefruit essential oil prepared by molecular distillation. *Molecules* **2020**, *25*, 217. [CrossRef]
57. Gefen, A.; Alves, P.; Beeckman, D.; Cullen, B.; Lázaro-Martínez, J.L.; Lev-Tov, H.; Santamaria, N.; Swanson, T.; Woo, K.; Söderström, B.; et al. Fluid handling by foam wound dressings: From engineering theory to advanced laboratory performance evaluations. *Int. Wound J.* **2024**, *21*, e14674. [CrossRef]
58. Barrera, L.A. Desarrollo de medicamentos biotecnológicos. Del laboratorio al paciente. *Medicina* **2018**, *40*, 44–55.
59. Steinhäuser, K.G.; Große Ophoff, M. The Need for Change: A Roadmap for the Sustainable Transformation of the Chemical Industry. *Sustain. Chem.* **2025**, *6*, 16. [CrossRef]
60. García-Sánchez, M.E.; Robledo-Ortiz, J.R.; Jiménez-Palomar, I.; González-Reynoso, O.; González-García, Y. Production of bacterial cellulose by *Komagataeibacter xylinus* using mango waste as alternative culture medium. *Rev. Mex. Ing. Química* **2020**, *19*, 851–865. [CrossRef]
61. Woods, G.L. Antibacterial susceptibility tests: Dilution and disk diffusion methods. In *Manual of Clinical Microbiology*, 7th ed.; Murray, P.R., Baron, E.J., Pfaller, M.A., Tenover, F.C., Yolken, R.H., Eds.; ASM Press: Washington, DC, USA, 1995; pp. 1327–1341.
62. *ISO 10993-12:2021*; Biological Evaluation of Medical Devices—Part 12: Sample Preparation and Reference Materials. International Organization for Standardization: Geneva, Switzerland, 2021.
63. *ISO 10993-5:2009*; Biological Evaluation of Medical Devices—Part 5: Tests for In Vitro Cytotoxicity. International Organization for Standardization: Geneva, Switzerland, 2009.
64. *ISO 10993-3:2014*; Biological Evaluation of Medical Devices—Part 3: Tests for Genotoxicity, Carcinogenicity and Reproductive Toxicity. International Organization for Standardization: Geneva, Switzerland, 2014.
65. Secretaría de Salud. *Medical Device Supplement to the Mexican Pharmacopoeia*, 4th ed.; Method MGA 0711 Pyrogen Test; Permanent Commission of the Pharmacopoeia of the United Mexican States: Mexico City, Mexico, 2017.
66. *ISO 10993-10:2010*; Biological Evaluation of Medical Devices—Part 10: Tests for Irritation and Skin Sensitization. International Organization for Standardization: Geneva, Switzerland, 2010.
67. Magnusson, B.; Kligman, A.M. The identification of contact allergens by animal assay. The guinea pig maximization test. *J. Investig. Dermatol.* **1969**, *52*, 268–276. [CrossRef]
68. Carreto, N.; Generalao, O.B.; Alguno, A.; Malaluan, R.; Lubguban, A.; Bautista, N.B.C.; Dumancas, G.G. Quantitative determination of sweet orange, lime, and grapefruit essential oil adulterants in lemon essential oil (*Citrus limon* L.) using attenuated total reflectance Fourier transform infrared spectroscopy and chemometrics. *J. Essent. Oil Res.* **2026**, *38*, 54–67. [CrossRef]
69. Bof, M.J.; Jiménez, A.; Locaso, D.E.; García, M.A.; Chiralt, A. Grapefruit Seed Extract and Lemon Essential Oil as Active Agents in Corn Starch—Chitosan Blend Films. *Food Bioprocess Technol.* **2016**, *9*, 2033–2045. [CrossRef]
70. Wang, W.; Bai, D.; Wu, C.; Li, H.; Xie, X.; Ji, W.; Gao, J. A Protocol for Constructing a Rat Wound Model of Type 1 Diabetes. *J. Vis. Exp.* **2023**, *192*, e64914. [CrossRef]
71. Mouro, C.; Gomes, A.; Gomes, A.P.; Gouveia, I.C. Sustainable Bacterial Cellulose Production Using Low-Cost Fruit Wastewater Feedstocks. *Nanomaterials* **2025**, *15*, 271. [CrossRef] [PubMed]
72. Gheorghita, D.; Grosu, E.; Robu, A.; Ditu, L.M.; Deleanu, I.M.; Pircalabioru, G.G.; Raiciu, A.D.; Bita, A.I.; Antoniac, A.; Antoniac, V.I. Essential Oils as Antimicrobial Active Substances in Wound Dressings. *Materials* **2022**, *15*, 6923. [CrossRef]
73. Pellegrino, R.; Lanzillotti, C.; Pollini, M.; Paladini, F. UV-Assisted Silver Functionalization of Cotton Gauze for Antimicrobial and Biocompatible Wound Healing Applications. *Microorganisms* **2026**, *14*, 213. [CrossRef]
74. Buriti, B.M.A.B.; Figueiredo, P.L.B.; Passos, M.F.; da Silva, J.K.R. Polymer-Based Wound Dressings Loaded with Essential Oil for the Treatment of Wounds: A Review. *Pharmaceuticals* **2024**, *17*, 897. [CrossRef]
75. Louis-Maerten, E.; Rodriguez Perez, C.; Cajiga, R.M.; Persson, K.; Elger, B.S. Conceptual foundations for a clarified meaning of the 3Rs principles in animal experimentation. *Anim. Welf.* **2024**, *33*, e39. [CrossRef]

76. *ISO 10993-1:2018*; Biological Evaluation of Medical Devices—Part 1: Evaluation and Testing Within a Risk Management Process. International Organization for Standardization: Geneva, Switzerland, 2018.
77. Yap, P.S.X.; Yusoff, K.; Lim, S.-H.E.; Chong, C.-M.; Lai, K.-S. Membrane Disruption Properties of Essential Oils—A Double-Edged Sword? *Processes* **2021**, *9*, 595. [CrossRef]
78. Qiu, Y.; Qiu, L.; Cui, J.; Wei, Q. Bacterial cellulose and bacterial cellulose-vaccarin membranes for wound healing. *Mater. Sci. Eng. C* **2016**, *59*, 303–309. [CrossRef]
79. Kołaczkowska, M.; Siondalski, P.; Kowalik, M.M.; Pęksa, R.; Długa, A.; Zając, W.; Malinowska-Pańczyk, E.; Sinkiewicz, I.; Staroszczyk, H.; Śliwińska, A.; et al. Assessment of the usefulness of bacterial cellulose produced by *Gluconacetobacter xylinus* E25 as a new biological implant. *Mater. Sci. Eng. C* **2019**, *97*, 302–312. [CrossRef] [PubMed]
80. Council of Europe. *European Pharmacopoeia*, 6th ed.; Council of Europe: Strasbourg, France, 2007.
81. Szymanski, L.; Gołaszewska, K.; Wiatrowska, A.; Dropik, M.; Krakowiak, P.; Małkowska, J.; Matak, D. Biocompatibility of novel albumin-aldehyde surgical adhesive. *Sci. Rep.* **2022**, *12*, 12749. [CrossRef] [PubMed]
82. Li, P.; Liu, S.; Yang, X.; Du, S.; Tang, W.; Cao, W.; Xing, X. Low-drug-resistance carbon quantum dots decorated injectable self-healing hydrogel with potent antibiofilm property and cutaneous wound healing. *Chem. Eng. J.* **2021**, *403*, 126387. [CrossRef]
83. *NOM-062-ZOO-1999*; Technical Specifications for the Production, Care and Use of Laboratory Animals. Diario Oficial de la Federación: Mexico City, Mexico, 2001.

Disclaimer/Publisher's Note: The statements, opinions and data contained in all publications are solely those of the individual author(s) and contributor(s) and not of MDPI and/or the editor(s). MDPI and/or the editor(s) disclaim responsibility for any injury to people or property resulting from any ideas, methods, instructions or products referred to in the content.